

A Theoretical Study on the Mechanism of Camphor Hydroxylation by Compound I of Cytochrome P450

Takashi Kamachi and Kazunari Yoshizawa*

Contribution from the Institute for Fundamental Research of Organic Chemistry,
Kyushu University, Fukuoka 812-8581, Japan

Received June 27, 2002; E-mail: kazunari@ms.ifoc.kyushu-u.ac.jp

Abstract: Mechanistic and energetic aspects for the conversion of camphor to 5-*exo*-hydroxycamphor by the compound I iron-oxo species of cytochrome P450 are discussed from B3LYP DFT calculations. This reaction occurs in a two-step manner along the lines that the oxygen rebound mechanism suggests. The activation energy for the first transition state of the H atom abstraction at the C5 atom of camphor is computed to be more than 20 kcal/mol. This H atom abstraction is the rate-determining step in this hydroxylation reaction, leading to a reaction intermediate that involves a carbon radical species and the iron-hydroxo species. The second transition state of the rebound step that connects the reaction intermediate and the product alcohol complex lies a few kcal/mol below that for the H atom abstraction on the doublet and quartet potential energy surfaces. This energetic feature allows the virtually barrierless recombination in both spin states, being consistent with experimentally observed high stereoselectivity and brief lifetimes of the reaction intermediate. The overall energetic profile of the catalytic mechanism of camphor hydroxylation particularly with respect to why the high activation energy for the H atom abstraction is accessible under physiological conditions is also considered and calculated. According to a proton source model involving Thr252, Asp251, and two solvent water molecules (*Biochemistry* **1998**, *37*, 9211), the energetics for the conversion of the iron-peroxo species to compound I is studied. A significant energy over 50 kcal/mol is released in the course of this dioxygen activation process. The energy released in this chemical process is an important driving force in alkane hydroxylation by cytochrome P450. This energy is used for the access to the high activation energy for the H atom abstraction.

1. Introduction

Cytochrome P450 enzymes ubiquitously distributed in living things play vital roles in the hydroxylation of endogenous, physiological substrates as well as a wide range of drugs and xenobiotics.¹ P450_{cam} discovered in *Pseudomonas putida* is the first soluble P450 enzyme purified in large quantities, and extensive investigations about it have been undertaken mainly by spectroscopic and X-ray crystallographic analyses.^{2,3} Many studies on the structures and functions of P450_{cam} lead to the proposed catalytic cycle, as depicted in Scheme 1.^{1,4} The resting form **1** of P450_{cam} is an inactive ferric species involving water as the sixth ligand. This water ligand is released to form the five-coordinate high-spin ferric species **2** when camphor is supplied to the heme pocket. This substrate binding triggers the electron transfer from putidaredoxin to the camphor complex,

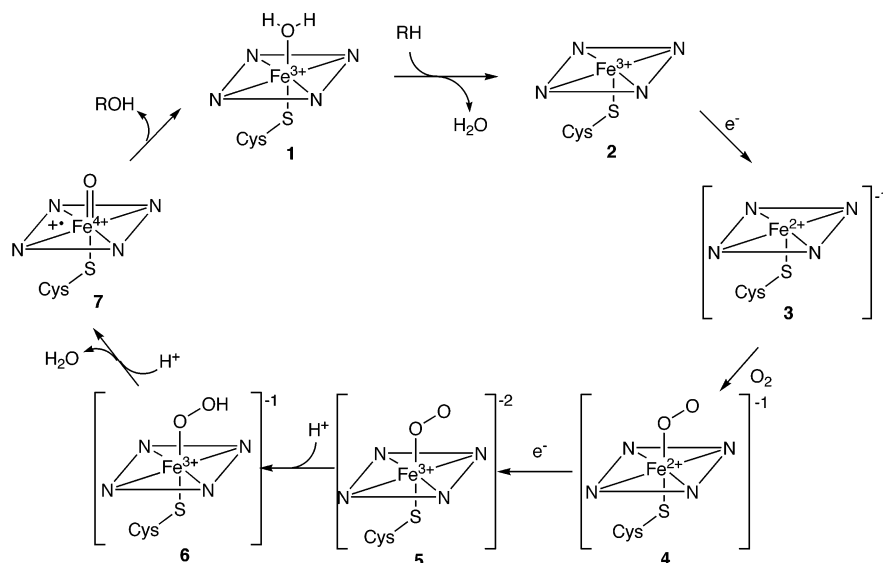
resulting in the five-coordinate ferrous complex **3**. Dioxygen is incorporated into this vacant coordination site of **3**, and as a result, the oxy intermediate **4** is generated. The ferric iron-peroxo species **5** is formed by the addition of a second electron to **4**, the rate-determining process in the catalytic cycle, and subsequently the ferric iron-hydroperoxo species **6** is generated by the protonation of the distal oxygen of **5**. Uptake of a second proton by the iron-hydroperoxo species would lead to the iron-oxo species **7**, which has a direct reactivity to substrate alkane. Owing to the recent development in transient-state crystallographic techniques, such species in the catalytic cycle of P450_{cam} were tentatively identified.⁵

P450_{cam} catalyzes the hydroxylation of camphor stereoselectively and regioselectively, leading to 5-*exo*-hydroxycamphor at more than 95% efficiency, as shown in Scheme 2. The iron-oxo species called compound I, which can be viewed as Fe^{IV}=O(Por⁺) or Fe^V=O(Por), is the most likely candidate for the oxygen source of the P450 family, in which Por is porphyrin. A generally accepted mechanism for hydrocarbon hydroxylation by P450 involves the initial H atom abstraction from a C–H bond of the substrate, followed by the recombination of the resultant radical species to form the hydroxylated product.^{6,7} Newcomb and co-workers estimated the lifetime of the radical

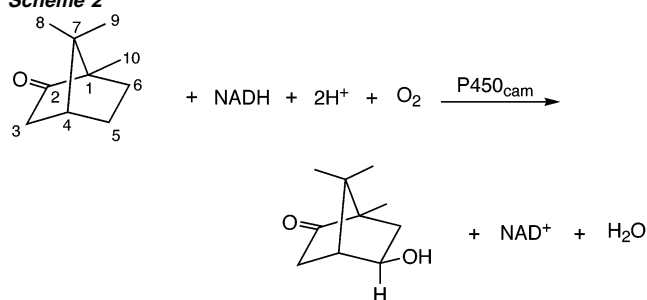
- (1) Reviews for example: (a) Sono, M.; Roach, M. P.; Coulter, E. D.; Dawson, J. H. *Chem. Rev.* **1996**, *96*, 2841. (b) *Cytochrome P-450: Structure, Mechanisms and Biochemistry*, 2nd ed.; Ortiz de Montellano, P. R., Ed.; Plenum: New York, 1995.
- (2) (a) Poulos, T. L.; Finzel, B. C.; Howard, A. J. *J. Mol. Biol.* **1987**, *195*, 687. (b) Poulos, T. L. *Adv. Inorg. Biochem.* **1988**, *7*, 1. (c) Poulos, T. L. *Curr. Opin. Struct. Biol.* **1995**, *5*, 767. (d) Poulos, T. L.; Finzel, B. C.; Gunsalus, I. C.; Wagner, G. C.; Kraut, J. *J. Biol. Chem.* **1985**, *260*, 16122.
- (3) (a) Davydov, R.; Macdonald, I. D. G.; Makris, T. M.; Sligar, S. G.; Hoffman, B. M. *J. Am. Chem. Soc.* **1999**, *121*, 10654. (b) Davydov, R.; Makris, T. M.; Kofman, V.; Werst, D. E.; Sligar, S. G.; Hoffman, B. M. *J. Am. Chem. Soc.* **2001**, *123*, 1403.
- (4) (a) Dawson, J. H.; Sono, M. *Chem. Rev.* **1987**, *87*, 1255. (b) Dawson, J. H. *Science* **1988**, *240*, 433.

- (5) Schlichting, I.; Berendzen, J.; Chu, K.; Stock, A. M.; Maves, S. A.; Benson, D. E.; Sweet, R. M.; Ringe, D.; Petsko, G. A.; Sligar, S. G. *Science* **2000**, *287*, 1615.

Scheme 1



Scheme 2



species using hypersensitive radical-clock substrates, which are able to differentiate between radical and cationic species in that different structural rearrangements occur for the two types of intermediates.⁸ Measured radical lifetimes of 80–200 fs are too short for the support of a real free radical intermediate, and the formation of cationic rearrangement products indicates the presence of a second oxidant iron-hydroperoxo species. Thus, their results raised a question about the prevailing oxidation mechanism of alkane hydroxylation mediated by P450, the so-called oxygen rebound mechanism.

Quantum chemical calculations have elucidated structural, electronic, and catalytic aspects of cytochrome P450. Loew and Harris investigated the validity of the proposed dioxygen activation pathways involving the protonation of the distal and proximal oxygen atoms of the iron-peroxo and iron-hydroperoxo species by density functional theory (DFT) computations.⁹ Shaik and co-workers have extensively studied the electronic states of various intermediates of P450 in detail^{10–14} and proposed

that the hydroxylation and epoxidation reactions should proceed in effectively concerted manners on the doublet potential energy surface, while the rebound step on the quartet potential energy surface requires significant activation energies to form the alcohol and epoxide products, which can lead to stereochemical scrambling.^{15–19} Our group calculated the kinetic isotope effect in the C–H bond dissociation of ethane to be in the range 7–13 at 300 K and supported that the hydrogen abstraction step is the rate-determining step in the catalytic cycle.²⁰ Recently, we studied dynamical aspects of this hydroxylation reaction from classical trajectory calculations and predicted the lifetimes for the radical intermediates to be about 200 fs under specific initial conditions.²¹ Moreover, Shaik et al. and our group investigated the oxygenation ability of the iron-hydroperoxo species, another candidate for the active species in olefin epoxidation.^{22,23} As a result of computations, the iron-hydroperoxo species was found to be an inactive intermediate, the reactivity of which is comparable to hydrogen peroxide itself, which exhibits no reactivity toward olefin.²³

In this paper, we describe the hydroxylation of camphor by a compound I model from DFT calculations. We present new aspects of this enzymatic reaction, in particular how a C–H bond of the substrate is activated and dissociated from the point

- (6) Groves, J. T.; Haushalter, R. C.; Nakamura, M.; Nemo, T. E.; Evans, B. J. *J. Am. Chem. Soc.* **1981**, *103*, 2884.
 (7) Groves, J. T. *J. Chem. Educ.* **1985**, *62*, 928.
 (8) (a) Newcomb, M.; Le Tadic, M. H.; Putt, D. A.; Hollenberg, P. F. *J. Am. Chem. Soc.* **1995**, *117*, 3312. (b) Newcomb, M.; Le Tadic-Biadatti, M. H.; Chestney, D. L.; Roberts, E. S.; Hollenberg, P. F. *J. Am. Chem. Soc.* **1995**, *117*, 12085. (c) Toy, P. H.; Newcomb, M.; Hollenberg, P. F. *J. Am. Chem. Soc.* **1998**, *120*, 7719. (d) Atkinson, J. K.; Hollenberg, P. F.; Ingold, K. U.; Johnson, C. C.; Le Tadic, M.-H.; Newcomb, M.; Putt, D. A. *Biochemistry* **1994**, *33*, 10630. (e) Newcomb, M.; Shen, R.; Choi, S.-Y.; Toy, P. H.; Hollenberg, P. F.; Vaz, A. D. N.; Coon, M. J. *J. Am. Chem. Soc.* **2000**, *122*, 2677.
 (9) (a) Loew, G. H.; Harris, D. L. *Chem. Rev.* **2000**, *100*, 407. (b) Harris, D. L.; Loew, G. H. *J. Am. Chem. Soc.* **1998**, *120*, 8941.
 (10) Filatov, M.; Harris, N.; Shaik, S. *Angew. Chem., Int. Ed.* **1999**, *38*, 3510.

- (11) Ogliaro, F.; Cohen, S.; Filatov, M.; Harris, N.; Shaik, S. *Angew. Chem., Int. Ed.* **2000**, *39*, 3851.
 (12) Ogliaro, F.; Cohen, S.; de Visser, S. P.; Shaik, S. *J. Am. Chem. Soc.* **2000**, *122*, 12892.
 (13) Ogliaro, F.; de Visser, S. P.; Groves, J. T.; Shaik, S. *Angew. Chem., Int. Ed.* **2001**, *40*, 2874.
 (14) Ogliaro, F.; de Visser, S. P.; Cohen, S.; Kaneti, J.; Shaik, S. *ChemBiochem* **2001**, *11*, 848.
 (15) Shaik, S.; Filatov, M.; Schröder, D.; Schwarz, H. *Chem. Eur. J.* **1998**, *4*, 193.
 (16) Filatov, M.; Harris, N.; Shaik, S. *J. Chem. Soc., Perkin Trans. 2* **1999**, 399.
 (17) Harris, N.; Cohen, S.; Filatov, M.; Ogliaro, F.; Shaik, S. *Angew. Chem., Int. Ed.* **2000**, *39*, 2003.
 (18) Ogliaro, F.; Harris, N.; Cohen, S.; Filatov, M.; de Visser, S. P.; Shaik, S. *J. Am. Chem. Soc.* **2000**, *122*, 8977.
 (19) de Visser, S. P.; Ogliaro, F.; Harris, N.; Shaik, S. *J. Am. Chem. Soc.* **2001**, *123*, 3037.
 (20) Yoshizawa, K.; Kagawa, Y.; Shiota, Y. *J. Phys. Chem. B* **2000**, *104*, 12365.
 (21) Yoshizawa, K.; Kamachi, T.; Shiota, Y. *J. Am. Chem. Soc.* **2001**, *123*, 9806.
 (22) Ogliaro, F.; de Visser, S. P.; Cohen, S.; Sharma, P. K.; Shaik, S. *J. Am. Chem. Soc.* **2002**, *124*, 2806.
 (23) Kamachi, T.; Shiota, Y.; Ohta, T.; Yoshizawa, K. *Bull. Chem. Soc. Jpn.*, in press.

of view of energetics. We consider and analyze a proton delivery system for the conversion of the iron-peroxo species to compound I to reveal the entire energy profile of dioxygen activation and alkane hydroxylation in the P450 catalytic cycle. The energy released in the course of the dioxygen activation process is a key to the access to the high activation energy for the C–H bond dissociation.

2. Model System and Method of Calculation

We used a six-coordinate complex $\text{Fe}^{4+}\text{O}^{2-}(\text{C}_{20}\text{N}_4\text{H}_{12})^{1-}(\text{SCH}_3)^{1-}$ as a compound I model of P450 and camphor as substrate. Thus, the total charge of the model reacting system is neutral. The program we used is the Gaussian 98 ab initio program package.²⁴ We calculated the energies and geometries of the reactants, intermediates, products, and transition states in the quartet and doublet spin states with the B3LYP method,²⁵ which consists of the Slater exchange, the Hartree–Fock exchange, the exchange functional of Becke,²⁶ the correlation functional of Lee, Yang, and Parr (LYP),²⁷ and the correlation functional of Vosko, Wilk, and Nusair.²⁸ For the Fe atom we used the triple- ζ -valence (TZV) basis set,²⁹ and for the H, C, N, O, and S atoms we used the D95 double- ζ basis set.³⁰ The combination of the B3LYP method and these basis sets is probably the best level of theory at present for the search of transition states about this “large” iron-porphyrin model. We refined the energies by single-point calculations with the following three basis sets. First, for Fe we used the (14s9p5d) primitive set of Wachters’ all-electron basis set with one polarization f-function ($\alpha = 1.05$), one diffuse s-function, two diffuse p-functions, and one diffuse d-function,^{31–33} for S we used the McLean–Chandler basis set³⁴ with one polarization d-function³⁵ and one diffuse s- and p-function,³⁶ and for other atoms we used the 6-311+G** basis set.^{37,38} Second, we used the compact effective potentials³⁹ (CEP) of Stevens, Basch, and Krauss with the [8s8p6d/4s4p3d] basis function for Fe and with the 1-2-1 “triple- ζ ” basis function (CEP-121G) for other atoms. Third, we used the double- ζ valence basis set (8s5p5d)/[3s3p2d]⁴⁰ with the ECP (effective core potential) replacing core electrons up to 2p for Fe, we used the double- ζ valence basis set (3s3p)/[2s2p] with the ECP for S,⁴¹ and we used the D95 double- ζ basis set³⁰ for other atoms. We call this combination of the basis sets LanL2DZ. We confirmed from systematic vibrational analyses that each transition state has only one

imaginary frequency mode. We calculated KIEs ($k_{\text{H}}/k_{\text{D}}$) from transition state theory with eq 1:⁴²

$$\frac{k_{\text{H}}}{k_{\text{D}}} = \left(\frac{m_{\text{D}}^R m_{\text{H}}^{\#}}{m_{\text{H}}^R m_{\text{D}}^{\#}} \right)^{3/2} \left(\frac{I_{\text{xD}}^R I_{\text{yD}}^R I_{\text{zD}}^R}{I_{\text{xH}}^R I_{\text{yH}}^R I_{\text{zH}}^R} \right)^{1/2} \left(\frac{I_{\text{xH}}^{\#} I_{\text{yH}}^{\#} I_{\text{zH}}^{\#}}{I_{\text{xD}}^{\#} I_{\text{yD}}^{\#} I_{\text{zD}}^{\#}} \right)^{1/2} \frac{q_{\text{vD}}^R q_{\text{vH}}^{\#}}{q_{\text{vH}}^R q_{\text{vD}}^{\#}} \times \exp\left(-\frac{E_{\text{H}}^{\#} - E_{\text{D}}^{\#}}{RT}\right) \quad (1)$$

where superscripts *R* and *#* specify the reactant camphor and the transition state for the H (D) atom abstraction, respectively, for the molecular mass *m*, the moment of inertia *I*, the vibrational partition function *q_v*, and the activation energy *E*. The last exponential term in this equation tells us that KIEs are temperature dependent. The numerator in the last exponential term comes from the fact that the C–H dissociation has a lower activation energy than the C–D dissociation on account of the former’s greater zero-point vibrational energy. We added Wigner tunneling corrections⁴³ to data obtained from transition-state theory.

3. Results and Discussion

Figure 1 shows a computed energy diagram and optimized geometries of the reaction intermediates and the transition states for the conversion of camphor to 5-*exo*-hydroxycamphor by a compound I model in the quartet and doublet spin states. Calculated atomic charges and spin densities for these reaction species are listed in Table 1. The general profiles of the energies and geometries are similar to those obtained in our previous study²⁰ in which ethane is oxidized as a substrate.

3.1. Reactant Complex. There is a debate with respect to the electronic structure of compound I with a thiolate ligand. Trautwein et al. reported from DFT X_{α} calculations that significant spin density is located on the sulfur atom of the CH_3S^- ligand instead of the porphyrin ring.⁴⁴ This trend was refined by higher-level DFT calculations at the B3LYP level of theory by Green⁴⁵ and Yoshizawa et al.⁴⁶ The calculated spin density distribution shown in Table 1 demonstrates that the $\text{Fe}=\text{O}$ moiety of the compound I model has two unpaired parallel-spin electrons, which are weakly coupled with one unit of spin mainly located on the thiolate ligand and partly located on the porphyrin ring. Shaik et al. demonstrated with the HS^- ligand that external factors such as medium polarization and hydrogen bonding between the sulfur atom and the NH group of amino acid residues can significantly reduce the spin density on the sulfur atom to form a porphyrin π cation radical species.^{12–14}

The doublet and quartet potential energy surfaces are close in energy in the course of the reaction. Although DFT calculations sometimes erroneously describe the spin-state energetics of porphyrins,⁴⁷ this does not significantly affect the essential energy profile because both potential energy surfaces are close in energy in the course of the reaction. In the initial stages of the reaction, the reaction camphor comes into contact with compound I to form a kind of encounter complex. Although there are various ways for binding, the hydroxylation of camphor

- (24) Frisch, M. J.; Trucks, G. W.; Schlegel, H. B.; Scuseria, G. E.; Robb, M. A.; Cheeseman, J. R.; Zakrzewski, V. G.; Montgomery, J. A.; Stratmann, R. E.; Burant, J. C.; Dapprich, S.; Millam, J. M.; Daniels, A. D.; Kudin, K. N.; Strain, M. C.; Farkas, O.; Tomasi, J.; Barone, V.; Cossi, M.; Cammi, R.; Mennucci, B.; Pomelli, C.; Adamo, C.; Clifford, S.; Ochterski, J.; Petersson, G. A.; Ayala, P. Y.; Cui, Q.; Morokuma, K.; Malick, D. K.; Rabuck, A. D.; Raghavachari, K.; Foresman, J. B.; Cioslowski, J.; Ortiz, J. V.; Stefanov, B. B.; Liu, G.; Liashenko, A.; Piskorz, Z.; Komaromi, I.; Gomperts, R.; Martin, R. L.; Fox, D. J.; Keith, T.; Al-Laham, M. A.; Peng, C. Y.; Nanayakkara, A.; Gonzalez, C.; Challacombe, M.; Gill, P. M. W.; Johnson, B.; Chen, W.; Wong, M. W.; Andres, J. L.; Gonzalez, C.; Head-Gordon, M.; Replogle, E. S.; Pople, J. A. *Gaussian 98*; Gaussian Inc.: Pittsburgh, PA, 1998.
- (25) Becke, A. D. *J. Chem. Phys.* **1993**, *98*, 5648.
- (26) Becke, A. D.; Roussel, M. R. *Phys. Rev. A* **1989**, *39*, 3761.
- (27) Lee, C.; Yang, W.; Parr, R. G. *Phys. Rev. B* **1988**, *37*, 785.
- (28) Vosko, S. H.; Wilk, L.; Nusair, M. *Can. J. Chem.* **1980**, *58*, 1200.
- (29) Schäfer, A.; Huber, C.; Ahlrichs, R. *J. Chem. Phys.* **1994**, *100*, 5829.
- (30) Dunning, T. H.; Hay, P. J. In *Modern Theoretical Chemistry*; Schaefer, H. F., III, Ed.; Plenum: New York, 1976; Vol. 3, p 1.
- (31) Wachters, A. J. H. *J. Chem. Phys.* **1970**, *52*, 1033.
- (32) Hay, P. J. *J. Chem. Phys.* **1977**, *66*, 4377.
- (33) Raghavachari, K.; Trucks, G. W. *J. Chem. Phys.* **1989**, *91*, 1062.
- (34) McLean, A. D.; Chandler, G. S. *J. Chem. Phys.* **1980**, *72*, 5639.
- (35) Francl, M. M.; Pietro, W. J.; Hehre, W. J.; Binkley, J. S.; Gordon, M. S.; DeFrees, D. J.; Pople, J. A. *J. Chem. Phys.* **1982**, *77*, 3654.
- (36) Frisch, M. J.; Pople, J. A.; Binkley, J. S. *J. Chem. Phys.* **1984**, *80*, 3265.
- (37) Krishnan, R.; Binkley, J. S.; Seeger, R.; Pople, J. A. *J. Chem. Phys.* **1980**, *72*, 650.
- (38) Clark, T.; Chandrasekhar, J.; Spitznagel, G. W.; Schleyer, P. v. R. *J. Comput. Chem.* **1983**, *4*, 294.
- (39) (a) Stevens, W. J.; Basch, H.; Krauss, M. *J. Chem. Phys.* **1984**, *81*, 6026. (b) Stevens, W. J.; Krauss, M.; Basch, H.; Jasien, P. G. *Can. J. Chem.* **1992**, *70*, 612.
- (40) Hay, P. J.; Wadt, W. R. *J. Chem. Phys.* **1985**, *82*, 299.

- (41) Wadt, W. R.; Hay, P. J. *J. Chem. Phys.* **1985**, *82*, 284.
- (42) McQuarrie, D. A. *Statistical Thermodynamics*; University Science Books: Mill Valley, 1973.
- (43) Wigner, E. *J. Chem. Phys.* **1937**, *5*, 720.
- (44) Antony, J.; Grodzicki, M.; Trautwein, A. X. *J. Phys. Chem. A* **1997**, *101*, 2692.
- (45) Green, M. T. *J. Am. Chem. Soc.* **1999**, *121*, 7939.
- (46) Ohta, T.; Matsuura, K.; Yoshizawa, K.; Morishima, I. *J. Inorg. Biochem.* **2000**, *82*, 141.
- (47) Scherlis, D. A.; Estrin, D. A. *Int. J. Quantum Chem.* **2002**, *87*, 158.

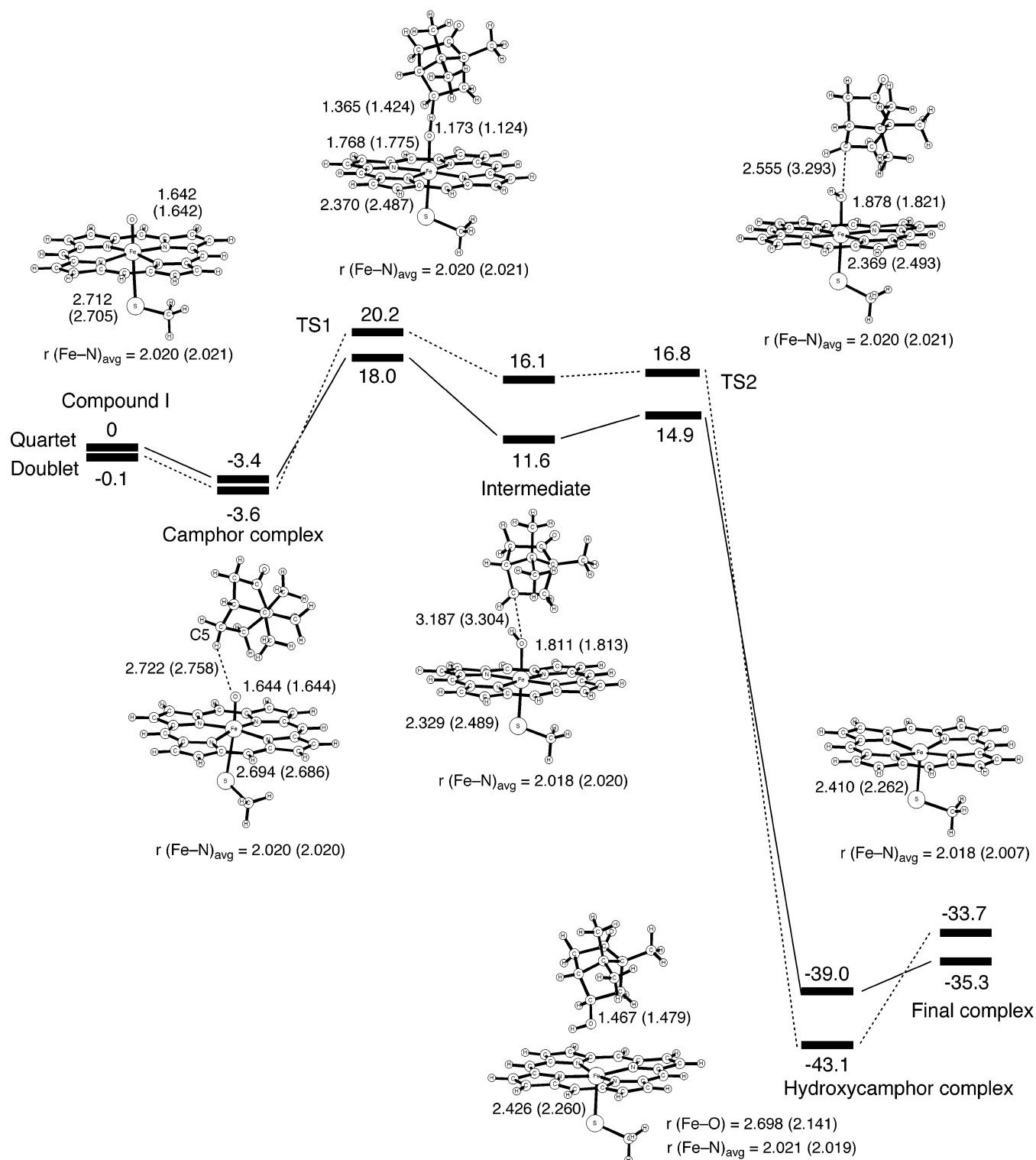


Figure 1. Computed energy diagram with optimized structures of the reaction species for camphor hydroxylation by a compound I model in the quartet (doublet) state. Bond distances in parentheses are for the doublet state. Energy in units of kcal/mol and bond distances in units of Å.

by P450_{cam} is a highly stereospecific and regioselective oxidation reaction that leads to 5-*exo*-hydroxycamphor.¹ As Table 2 shows, computed energies of various camphor radicals demonstrate that the order of total energy is C3 \ll C6 < C5 < C9 < C8 \approx C10 < C4 (see Scheme 2). Therefore the C3 radical is energetically the most stable species and the C6 and C5 radicals are the second and third most stable species, respectively, although 5-*exo*-hydroxycamphor is nearly 100% produced in this reaction.

Indeed, the P450-mediated hydroxylation of a camphor analogue norcamphor, which has a more loose affinity to the binding site of P450, forms more stable products 3-*exo*-hydroxynorcamphor (8%), 6-*exo*-hydroxynorcamphor (47%), and 5-*exo*-hydroxynorcamphor (45%).⁴⁷ These facts suggest that the coordination of the substrate to the catalytic active site is a key to the selective hydroxylation at C5 of camphor. Poulos et al. first reported the detailed structure of a camphor-binding pocket² and demon-

Table 1. Calculated Mulliken Charges and Spin Densities for the Fe and O Atoms and the CH₃S and Porphyrin (Por) Moieties (values in parentheses are spin densities)

	doublet state				quartet state			
	Fe	O	CH ₃ S	Por	Fe	O	CH ₃ S	Por
compound I	1.1 (1.2)	-0.4 (0.9)	0.0 (-0.8)	-0.7 (-0.3)	1.1 (1.2)	-0.4 (0.9)	0.0 (0.8)	-0.7 (0.1)
camphor complex	1.1 (1.3)	-0.4 (0.8)	0.0 (-0.8)	-0.7 (-0.3)	1.1 (1.2)	-0.4 (0.9)	0.0 (0.8)	-0.7 (0.1)
TS1	1.1 (0.9)	-0.3 (0.5)	0.0 (-0.7)	-0.7 (-0.3)	1.1 (1.4)	-0.2 (0.6)	-0.1 (0.4)	-0.7 (0.0)
intermediate	1.1 (1.0)	-0.3 (0.1)	0.0 (-0.7)	-0.8 (-0.4)	1.1 (1.8)	-0.3 (0.3)	-0.1 (0.1)	-0.7 (-0.2)
TS2	1.1 (1.0)	-0.3 (0.1)	0.0 (-0.7)	-0.8 (-0.3)	1.1 (2.1)	-0.3 (0.0)	-0.3 (0.2)	-0.6 (-0.2)
hydroxycamphor complex	1.0 (1.0)	-0.2 (0.0)	-0.2 (0.1)	-0.9 (-0.1)	1.2 (2.5)	-0.2 (0.0)	-0.3 (0.5)	-0.9 (0.0)
final complex	1.0 (1.2)	-0.2 (0.0)	-0.2 (-0.1)	-0.8 (-0.1)	1.2 (2.5)	-0.2 (0.0)	-0.3 (0.5)	-0.9 (0.0)

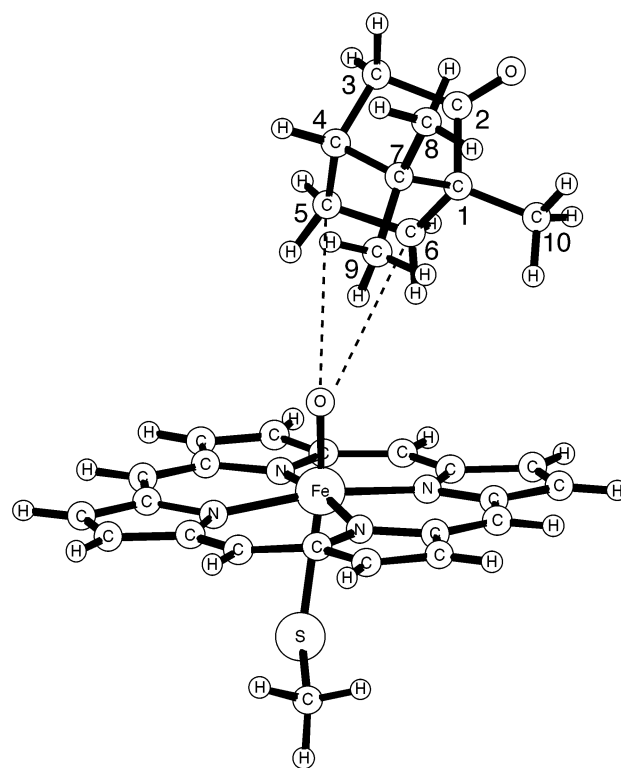
Table 2. Relative Energies of Radicals and Relative Probability of Radical Production in Camphor

position and radical type ^a	relative energy ^b (kcal/mol)	relative probability of radical production ^c
C3 (2°)	0.0	1.0
C4 (3°)	15.5	4.9 × 10 ⁻¹²
C5 (2°)	7.4	4.1 × 10 ⁻⁶
C6 (2°)	5.0	2.1 × 10 ⁻⁴
C8 (1°)	9.3	1.8 × 10 ⁻⁷
C9 (1°)	9.1	2.4 × 10 ⁻⁷
C10 (1°)	9.3	1.6 × 10 ⁻⁷

^a 1°, 2°, and 3° indicate primary, secondary, and tertiary radicals, respectively. ^b Relative to the energy of the C3 radical. ^c Calculated with the Boltzmann distribution.

strated that Tyr96 plays a major role in positioning the substrate through the hydrogen bond between the hydroxyl group of Tyr96 and the carbonyl oxygen atom of camphor. For example, when the carbonyl oxygen atom of camphor is replaced by sulfur, the relative yield of 5-*exo*-hydroxycamphor significantly decreases to 64%, due to the perturbation in this hydrogen bond.⁴⁸ Val295 is also essential to stereospecific substrate binding via the interaction between the valine side chain and the C8 and C9 methyl groups. Thus, the protein environment in cytochrome P450_{cam} plays an essential role in the binding of camphor to the active site and the selective hydroxylation. Figure 2 shows that the *exo* face of the C5 atom of camphor is oriented toward the iron atom and close to the oxygen atom of compound I. If this layout of substrate is realized in the protein environment, it would permit the selective H atom abstraction at C5 and the resultant conversion of camphor to 5-*exo*-hydroxycamphor, despite its energetic unstability compared to the C3 and C6 camphor radicals.

3.2. C–H Bond Activation Process. The transition state for the H atom abstraction (TS1) at the C5 atom of camphor is presented in Figure 1. It has an O–H bond of 1.173 (1.124) Å and a C–H bond of 1.365 (1.424) Å in the quartet (doublet) state; these bond distances as well as a linear arrangement of the C–H–O moiety are a typical feature in the C–H bond activation by various FeO species.⁵⁰ The activation energy for the H atom abstraction at C5 is 21.4 (23.8) kcal/mol in the

**Figure 2.** Selected bond distances of the camphor complex in the quartet and doublet states. Bond distances in parentheses are for the doublet state. Values in units of Å.

quartet (doublet) state. This energy is smaller than that for the C–H bond cleavage of ethane 22.0 (28.6) kcal/mol in the quartet (doublet) state, but it is still large. Interactions of the active site model with protein are not taken into account, and this environmental effect may have an impact on the relative energies and the charge (spin) distribution. Recently, Shaik et al. reported from QM/MM calculations that the inclusion of hydrogen bonds to the axial ligand transforms the electronic structure of compound I from a sulfur-centered radical to a porphyrin-centered radical cation.⁵¹ They showed that the FeO unit still has a spin density of about 2.0 even if the electronic structure is changed, like in our compound I model (see Table 1). Since the reactivity of compound I is likely to depend on the radical character of the FeO unit, the activation energy of this H atom abstraction is expected to be almost unchanged.

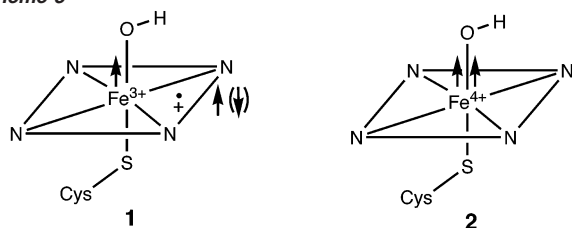
(48) Atkins, W. M.; Sligar, S. G. *J. Am. Chem. Soc.* **1987**, *109*, 3754.

(49) Atkins, W. M.; Sligar, S. G. *J. Biol. Chem.* **1988**, *263*, 18842.

(50) (a) Yoshizawa, K.; Shiota, Y.; Yamabe, T. *Organometallics* **1998**, *17*, 2825.

(b) Yumura, T.; Yoshizawa, K. *Organometallics* **2001**, *20*, 1397. (c) Ohta, T.; Kamachi, T.; Shiota, Y.; Yoshizawa, K. *J. Org. Chem.* **2001**, *66*, 4122.

Scheme 3



The transition state TS1 leads to the formation of an intermediate cluster, where the iron-hydroxo species and the camphor radical are weakly bound through the interaction between the hydroxo group and the C5 atom. The distance between the oxygen atom of the hydroxo group and the C5 atom is 3.187 and 3.304 Å in the doublet and quartet states, respectively. Since a calculated atomic charge (spin density) at C5 is 0.0 (1.0) in both spin states, we can reasonably rule out mechanisms involving carbanions and carbocations. Thus, the C–H bond of the substrate is homolytically cleaved. The iron-hydroxo species can exist in two different forms; the first one is the Fe^{3+} state with porphyrin π -cation radical **1** and the second one is the Fe^{4+} state with closed-shell porphyrin **2**, as indicated in Scheme 3. On the doublet potential energy surface, the H atom abstraction is accompanied with the reduction of the iron atom to produce the Fe^{3+} state, the spin density of which was calculated to be 1.0 on the iron atom, 0.1 on the oxygen atom, -0.7 on the CH_3S ligand, and -0.4 on the porphyrin ring. In contrast, on the quartet surface the Fe^{4+} state is formed by the reduction of the porphyrin ring instead of the iron atom. The spin density in the Fe^{4+} state was calculated to be 1.8 on the iron atom, 0.3 on the oxygen atom, 0.1 on the CH_3S ligand, and -0.2 on the porphyrin ring. Our B3LYP calculations showed that the Fe^{3+} state lies 5.0 kcal/mol above the Fe^{4+} state. We considered effects of the protein environment in the heme pocket using the PCM model ($\epsilon = 5.6$),⁵² which can generally reproduce the electrostatic field environment of the protein.^{11–14} However, this effect does not change the energetic order of these species. Thus, the Fe^{4+} state is more stable than the Fe^{3+} state in energy in this reaction species.

3.3. Transition State for the Rebound Process. Figure 3 shows optimized geometries of the transition state for the recombination of the C5 camphor radical and the iron-hydroxo species (TS2), the so-called rebound step, as well as the corresponding imaginary modes of vibration. This transition state correctly leads to the alcohol complex. We successfully located the transition state for this important step on the potential energy surfaces of both doublet and quartet states. Our calculations demonstrated that the transition state in the doublet state has a 0.7 kcal/mol barrier for the C–H bond cleavage. However, the doublet rebound pathway is energetically very flat and it is substantially barrierless, which is in good agreement with Shaik's conclusion that the transition state for the rebound step does not exist and this process is virtually barrierless on the low-spin doublet potential energy surface, while the transition state for this step lies 5 kcal/mol above the iron-hydroperoxo

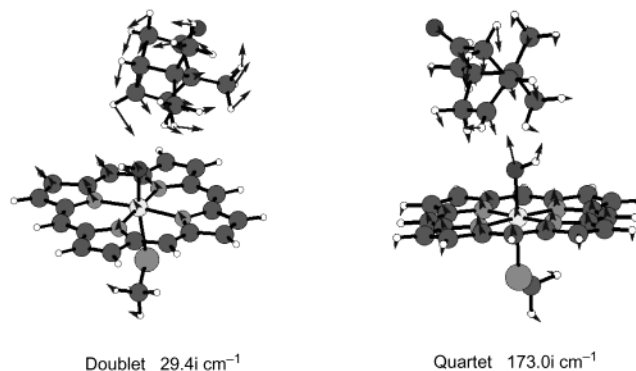
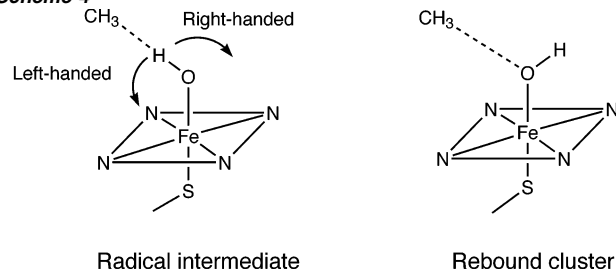


Figure 3. Imaginary modes of TS2 in the doublet and quartet states.

Scheme 4



species on the high-spin quartet surface.^{17,18} Recent theoretical studies^{18,21,53} for the hydroxylation of methane as a model of substrate suggested that the rotation of the OH group occupying the sixth ligand position is important before the recombination of methyl radical and the OH group, as shown in Scheme 4. Shaik et al. reported that a methyl migration first takes place and orients the methyl group toward the vacant site of the hydroxo group, leading to the “rebound cluster” where the C–O–Fe–H dihedral angle is 180° .¹⁸ These DFT calculations tell us that this rotational process is endothermic by about 1 kcal/mol. Hata et al. discussed this rotational motion in detail and demonstrated that this process is endothermic by 2 kcal/mol, and the activation energy for the left-handed rotation is 3 kcal/mol and that for the right-handed rotation is 5 kcal/mol.⁵³ Their calculations predicted that the barrier for the rebound process is only 1 kcal/mol. Moreover, our previous dynamical study for the hydroxylation of ethane showed that ethyl radical recombines with the hydroxo ligand to form the ethanol complex when the rotational mode of the OH group is effectively activated.²¹ Our results suggest that the transition state for the rebound step has C–O–Fe–H dihedral angles of 119.0° and 158.0° in the doublet and quartet states, respectively, and this geometrical layout permits a significant interaction between the unpaired p orbital of the radical center and the nonbonding electron pair of the hydroxo ligand.

Figure 3 shows the imaginary vibrational mode with respect to TS2 in both spin states. It is useful to look at the imaginary mode of vibration about a transition state because it can give us important information concerning the reaction coordinate. The imaginary mode of TS2 in the doublet state ($29.4i \text{ cm}^{-1}$) includes rotational motion of the OH group as well as stretching motion of the C–O bond being formed. The rotational motion of the C5 camphor radical which brings about the association of the radical species to the iron-hydroperoxo

(51) Schöneboom, J. C.; Lin, H.; Reuter, N.; Thiel, W.; Cohen, S.; Oglario, F.; Shaik, S. *J. Am. Chem. Soc.* **2002**, *124*, 8142.

(52) (a) Miertus, S.; Scrocco, E.; Tomasi, J. *Chem. Phys.* **1981**, *55*, 117. (b) Miertus, S.; Tomasi, J. *J. Chem. Phys.* **1982**, *65*, 239. (c) Barone, V.; Cossi, M.; Tomasi, J. *J. Chem. Phys.* **1997**, *107*, 3210. (d) Cossi, M.; Barone, V.; Cammi, R.; Tomasi, J. *Chem. Phys. Lett.* **1996**, *225*, 327.

(53) Hata, M.; Hirano, Y.; Hoshino, T.; Tsuda, M. *J. Am. Chem. Soc.* **2001**, *123*, 6410.

Table 3. Calculated Single-Point Energies (kcal/mol) of TS1, Reaction Intermediate, and TS2 with Various Basis Sets

basis set	TS1	reaction intermediate	TS2
LanL2DZ	5.4 (4.8)	0.0 (−0.6)	2.5 (0.0)
CEP-121G	8.1 (9.3)	0.0 (3.0)	2.9 (3.7)
6-311+G**	11.2 (13.0)	0.0 (3.6)	2.9 (4.3)

^a All values are relative to the energy of the reaction intermediate in the quartet state in each basis set.

in this mode. We carried out preliminary molecular dynamics simulations with respect to this rebound process to look at whether the transition-state structure correctly connects the reaction intermediate and the product alcohol complex. We supplied a small amount of kinetic energy (0.1 kcal/mol) to this transition state toward the forward and backward directions and confirmed that TS2 correctly connects the reaction intermediate and the product complex.⁵⁴ In the quartet state, a relatively high energy of 3.3 kcal/mol is needed to pass over the activation barrier of TS2. The increase in the activation energy in the quartet state changes the transition-state structure to a more product-like structure, the C–O (Fe–O) bond length being 2.555 (1.878) Å in the quartet state. This transition state has only one imaginary frequency mode of 173.0i cm^{−1}, which corresponds to the C–O stretching and the OH group rotation.

3.4. Mechanistic Features of Camphor Hydroxylation. The C–O–Fe–H dihedral angle of the reaction intermediate was calculated to be 28.6° and 24.8° in the doublet and quartet states, respectively. This structural deviation from the linear C–H–O arrangement should lead to the left-handed rotation with a lower activation energy. In both spin states, the transition state for the rebound step (TS2) lies energetically below that for the H atom abstraction (TS1), which is the rate-determining step. This energetic feature allows the virtually barrierless recombination in both spin states, being consistent with experimentally observed high stereoselectivity in this reaction⁵⁵ and brief lifetimes of the reaction intermediate.⁸ The quartet state lies below the doublet state in TS1, in the reaction intermediate, and in TS2, which is also seen in our previous study of ethane hydroxylation at the same level of theory.²⁰ However, the quartet state lies above the doublet state in our previous calculations at the B3LYP/3-21G level of theory.²¹ To see which is correct, we carried out single-point calculations with the LanL2DZ, CEP-121G, and 6-311+G** basis sets and list computational results in Table 3. These data clearly show that the lower-level calculations with the 3-21G and LanL2DZ basis sets erroneously predicted the energetical order in the doublet and quartet states, in contrast to the higher-level calculations with the CEP-121G and 6-311+G** basis sets.

Kinetic isotope effect (KIE) (k_H/k_D) is an important measure in general in discussing how the electronic process for the H atom abstraction of substrate hydrocarbon takes place in catalytic and enzymatic reactions.^{56,57} Table 4 lists computed k_H/k_D values for the H atom abstraction at C5 of camphor. The k_H/k_D value for the H atom abstraction at 300 K was calculated to be 7.07

(54) We used the velocity Verlet algorithm for propagating the nuclei classically and took a time interval of 0.5 fs. The forces were analytically calculated with the B3LYP method. See ref 21.

(55) Gelb, M. H.; Heimbrosk, D. C.; Mällkönen, P.; Sligar, S. G. *Biochemistry* **1982**, *21*, 370.

(56) Hjelmeland, L. M.; Aronow, L.; Trudell, J. R. *Biochem. Biophys. Res. Commun.* **1977**, *76*, 541.

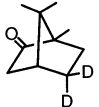
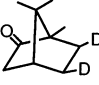
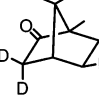
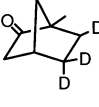
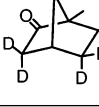
(57) Groves, J. T.; McClusky, G. A.; White, R. E.; Coon, M. J. *Biochem. Biophys. Res. Commun.* **1978**, *81*, 154.

Table 4. k_H/k_D Values in the H Atom Abstraction at the 5-*exo* Position of Camphor by a Compound I Model

T (K)	quartet		doublet	
	TST	TST/W	TST	TST/W
200	18.46	29.15	17.89	25.46
250	10.38	15.64	10.24	13.83
300	7.10	10.21	7.07	9.11
350	4.93	6.80	4.94	6.13
400	4.39	5.83	4.41	5.30
450	3.73	4.78	3.76	4.39
500	3.26	4.06	3.28	3.76

^a TST: transition-state theory. TST/W: TST with Wigner tunneling correction.

Table 5. k_H/k_D Values in the H Atom Abstraction at the 5-*exo* Position of Deuterated Camphors by a Compound I Model

Substrate	Quartet		Doublet	
	TST	TST/W	TST	TST/W
	8.58	12.50	8.54	11.15
	6.01	8.65	7.40	9.55
	13.18	18.95	7.10	9.16
	6.61	9.62	8.94	11.66
	12.88	18.52	7.44	9.60

^a TST: transition-state theory. TST/W: TST with Wigner tunneling correction.

and 7.10 in the doublet and quartet states, respectively. The values are increased to 9.11 and 10.21 with Wigner tunneling corrections in the doublet and quartet states, respectively. The intramolecular isotope effect for camphor hydroxylation is not exactly determined because the H atom abstraction can occur from either the *exo* or *endo* position at C5.⁵⁵ The values listed in Table 4 are typical of the kinetic isotope effects observed for P450-catalyzed hydroxylation reactions.^{56,57} For example, Groves et al. studied the P450-mediated hydroxylation of norbornane, which is structurally similar to camphor, and found the k_H/k_D value for this reaction to be 11.5. This large value is fully consistent with the homolytic C–H bond dissociation.⁵⁷ Moreover, we investigated the change of KIE by the specific deuteration of the camphor skeleton at the 3-, 5-, and 6-positions. Table 5 clearly shows that the k_H/k_D values are significantly affected by molecular parts that have no direct relevance to the abstraction reaction. Interestingly, the k_H/k_D values of the deuterated camphors are sensitive to the spin state of compound I. The results of 5-*exo*-camphor-3,3,5-*d*₃ and camphor-3,3,5,5-*d*₄ indicate that the kinetic isotope effect is greatly increased in

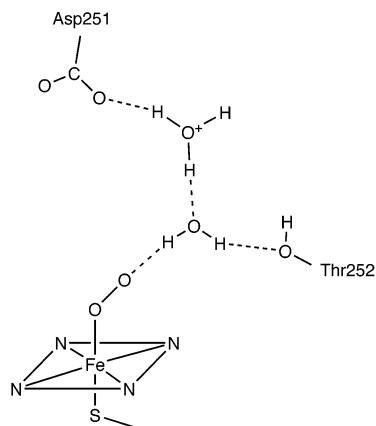


Figure 4. Proton delivery model for P450_{cam} proposed by Sligar et al.⁶²

the quartet state by the deuteration of the 3-position of camphor, while it remains unchanged in the doublet state. Measurements of KIE using these deuterated camphors are probably helpful in investigating whether the H atom abstraction proceeds in the doublet or quartet state on the basis of this drastic change in KIE.

3.5. Role of Dioxygen Activation in the Overall Catalytic Cycle. The calculated activation energy for the H atom abstraction is rather high (~ 20 kcal/mol) for an enzymatic reaction, and TS1 is energetically the highest species on the reaction pathway presented in Figure 1. In view of this quantity, the C–H bond activation by compound I is unlikely to occur under physiological conditions. However, the overall rate-determining step in the catalytic cycle shown in Scheme 1 is the reduction of **4** to **5**, and after this step camphor is immediately converted to 5-*exo*-hydroxycamphor.⁵⁸ For this reason, it is important to study the energy profile of dioxygen activation in the P450 catalytic cycle, which is just a prior step of camphor hydroxylation. Compound I is formed by the protonation of the iron-peroxy and iron-hydroperoxy intermediates; however, the proton delivery mechanism for the O–O bond scission is not clear at present because there is no obvious proton source unlike the distal histidine of peroxidases.⁵⁹ The mutation of Thr252 in P450_{cam} results in a significant decrease of hydroxylation ability,⁶⁰ and the replacement of Asp251 with Asn decreases the overall rate of the reaction.⁶¹ Moreover, a proton inventory analysis of experimental kinetic solvent isotope effect (KSIE) data indicates that at least two protons are involved in the formation of compound I.⁶² Sligar et al. proposed a possible proton delivery model for P450_{cam} involving Thr252, Asp251, and solvent water,⁶² as shown in Figure 4. These amino acid residues and solvent water form a hydrogen-bonding network that connects with the distal oxygen atom of the dioxygen ligand of the iron-peroxy intermediate.

Harris and Loew investigated from DFT calculations a proton-assisted pathway for the formation of compound I.⁹ They showed that the addition of a first proton to the distal oxygen atom of the iron-peroxy species is a highly exothermic reaction with $\Delta E = -422$ kcal/mol, and the protonation of the iron-

hydroperoxy species which leads to the formation of compound I and water is also a highly exothermic reaction with $\Delta E = -334$ kcal/mol. These large heats of reaction are mainly due to the neglect of the protein environment in the binding site. Naked protons which have a very strong affinity toward other molecules were assumed to be added to the distal oxygen atom of the peroxy and hydroperoxy intermediates in their calculations. Such a model will overestimate the heats of reaction. We performed DFT calculations to look at roles of the protein environment in the formation of compound I.

Here we adopted the proton source model of Sligar et al.⁶² that involves Thr252, Asp251, and two solvent water molecules as well as the iron-porphyrin complex, as depicted in Figure 5. At first, we calculated the oxy intermediate **4** on the basis of the X-ray structure (pdbcode:1DZ8). Only the singlet state was examined because previous studies⁶³ reported that this state is the energetically lowest one for the oxy complex. Geometry optimization was carried out with the constraints on the positions of all heavy atoms in Thr252 and Asp251 and in the porphyrin ring to retain the X-ray structure in the absence of the protein environment. Because of the very heavy computational task for this large system, we used the STO-3G basis set⁶⁴ for the porphyrin ligand and the methyl group of the axial ligand in the geometry optimization and we finally performed single-point calculations using the D95 basis set. The second electron donation to this species leads to the iron-peroxy species, and the subsequent proton transfer produces the iron-hydroperoxy and -oxo species. The iron-peroxy species barrierlessly collapses to the iron-hydroperoxy species during the geometry optimization process, and therefore we estimated the energy of the iron-peroxy species from a single-point calculation at the optimized structure of the oxy complex. These transient intermediates involve a complex hydrogen-bonding network in which protons are transferred through the amino acid residues and two solvent water molecules. The proton transfer is triggered by the reduction of the oxy complex which has protonated Asp251 at an end of the proton-donating pathway, and this is transferred to the oxygen atom of the adjacent water. This protonated water, in turn, delivers a proton to the other water that is hydrogen bonded to the distal oxygen atom of the iron-peroxy species. The selective proton donation to the distal oxygen atom from the second protonated water finishes with the formation of the iron-hydroperoxy species.

The proton delivery system also plays an important role in the O–O bond activation of the iron-hydroperoxy species. The distal oxygen atom of the iron-hydroperoxy species is hydrogen bonded to a water molecule and the OH group of Thr252, and these hydrogen bond networks promote the effective proton donation to the distal oxygen of the iron-hydroperoxy species. Our calculation revealed that the leading candidate for the proton source in this step is the hydroxyl group of Thr252 because this amino acid residue has an acidic hydrogen atom that is nearest to the distal oxygen atom of the iron-hydroperoxy model complex and the proton transfer from the neighboring water molecule is energetically unfavorable in comparison with Thr252.

The conversion of the iron-peroxy species to the iron-hydroperoxy species was computed to be 53.9 (50.1) kcal/mol

(58) Brewer, C. B.; Peterson, J. A. *J. Biol. Chem.* **1988**, *263*, 791.

(59) Poulos, T. L.; Kraut, J. *J. Biol. Chem.* **1980**, *255*, 8199.

(60) Martinis, S. A.; Atkins, W. M.; Stayton, P. S.; Sligar, S. G. *J. Am. Chem. Soc.* **1989**, *111*, 9252.

(61) Benson, D. E.; Suslick, K. S.; Sligar, S. G. *Biochemistry* **1997**, *36*, 5104.

(62) Vidakovic, M.; Sligar, S. G.; Li, H.; Poulos, T. L. *Biochemistry* **1998**, *37*, 9211.

(63) Harris, D.; Loew, G.; Waskell, L. *J. Am. Chem. Soc.* **1998**, *120*, 4308.

(64) Hehre, W. J.; Stewart, R. F.; Pople, J. A. *J. Chem. Phys.* **1969**, *51*, 2657.

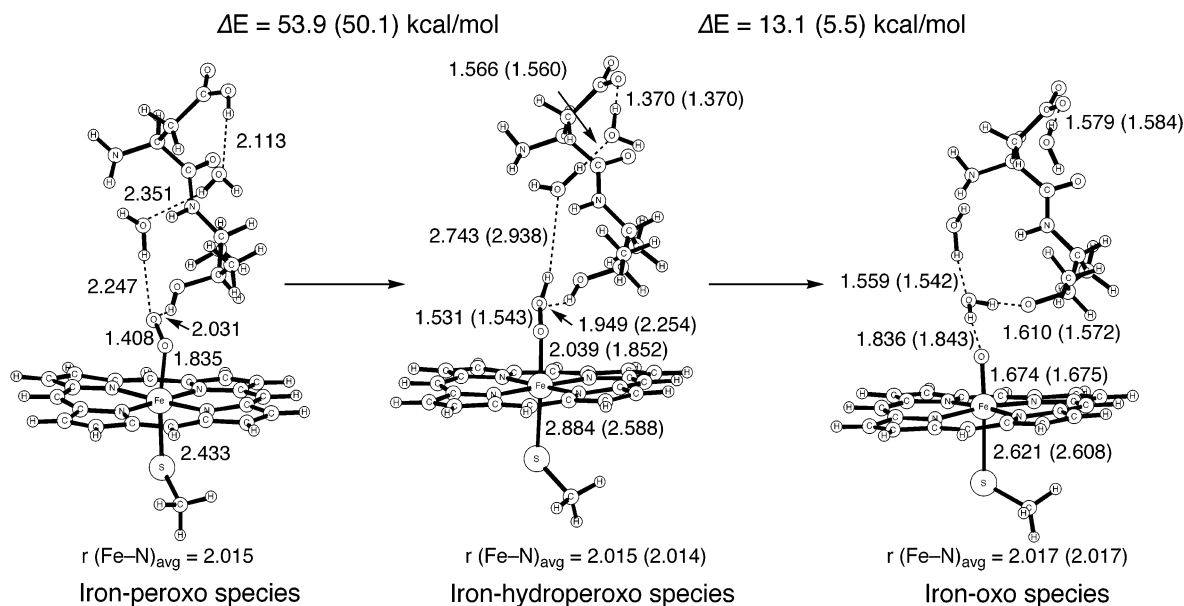


Figure 5. Computed energetical change in the dioxygen activation process after the formation of the reduced ferrous dioxygen species. Bond distances and energies in parentheses are for the doublet state. Energy in units of kcal/mol and bond distances in units of Å.

exothermic in the quartet (doublet) spin state. These values are smaller than Harris and Loew's value (422 kcal/mol),⁹ due to the stabilization of the proton in the hydrogen-bond network between amino acid residues in the binding pocket. Recently, Guallar et al. investigated a proton-transfer system in the dioxygen activation process of cytochrome P450eryF, in which a stable network of hydrogen bonds is formed among Ser246, two water molecules, and the distal oxygen atom of the dioxygen ligand of the iron-peroxo complex.⁶⁵ According to their proposal, the proton transfer effectively occurs when the iron-peroxo species is formed by the reduction of the oxyferrous species in the doublet state. They predicted this process to be only 10.7 kcal/mol exothermic in the addition of the first proton to the distal oxygen atom at the active site of P450_{cam}. An underlying reason is the difference of models adopted for the proton delivery system. For example, the production of unstable OH⁻ species in the proton-transfer mechanism by Guallar et al. cancels the stabilization of the active site model by the formation of the more stable iron-hydroperoxo species,⁶⁵ whereas the proton delivery in our calculations based on the proposal of Sligar et al.⁶² should be more exothermic because the proton is supplied from more acidic Asp251. There are a few proposals for the dioxygen activation mechanism such as a direct proton donation from the hydroxyl group of Thr252.⁶⁶ This model might bring about more mild proton donation to the distal oxygen atom of the dioxygen ligand. We computed the second protonation process from the iron-hydroperoxo species to compound I and water to be only 13.1 (5.5) kcal/mol exothermic in the quartet (doublet) state. Figure 5 shows the energetic profile of the dioxygen activation process after the formation of the reduced ferrous dioxygen species **5**. A significant energy over 50 kcal/mol is released in this process. Although the protein pocket, of course, partially absorbs this excess energy released in the proton delivery process, these transient intermediates can decay before complete equilibration of the system, and this

energy is in part used to pass over the potential energy barrier for the H atom abstraction by compound I. For these reasons, dioxygen activation is an essential driving force in alkane hydroxylation mediated by P450. Considering this important feature is essential in designing functional P450 model systems that are able to activate the inert C–H bonds of alkanes because alkane hydroxylation is directly related to the dioxygen activation process in energy.

4. Conclusions

We presented new DFT results on the hydroxylation of camphor by a compound I model of cytochrome P450. The activation energy for the transition state of the H atom abstraction is 21.4 (23.8) kcal/mol in the quartet (doublet) state, the values of which are nearly identical to those of the hydroxylation of ethane. The H atom abstraction is the rate-determining step, leading to the reaction intermediate involving a carbon radical species and the iron-hydroxo species. The transition state of the rebound step is located on the doublet and quartet potential energy surfaces. The calculated activation energy in the quartet state is 3.3 kcal/mol, while that in the doublet state is 0.7 kcal/mol. The imaginary vibrational mode of this transition state is characterized by rotational motion of the OH group as well as stretching motion of the C–O bond. The small barrier in the doublet state would come from the rotational motion of the OH group to cleave the weak interaction between the carbon radical center of the C5 camphor radical and the hydrogen atom of the hydroxo ligand. In both spin states, the transition state for the rebound step lies energetically below that for the H atom abstraction. Therefore the virtually barrierless recombination occurs in both spin states, resulting in experimentally observed high stereoselectivity and brief lifetimes of the reaction intermediate. The calculated k_H/k_D value for the H atom abstraction at C5 of camphor at 300 K is 7.07 and 7.10 in the doublet and quartet states, respectively, these values being

(65) Guallar, V.; Harris, D. L.; Batista, V. S.; Miller, W. H. *J. Am. Chem. Soc.* **2002**, *124*, 1430.

(66) Aikens, J.; Sligar, S. G. *J. Am. Chem. Soc.* **1994**, *116*, 1143.

typical of the kinetic isotope effects observed in P450-catalyzed hydroxylation reactions. Finally, on the basis of the model of Sligar et al., we considered the proton delivery mechanism to understand the entire energy profile of dioxygen activation in the P450 catalytic cycle. The overall catalytic pathways after the reduction of the ferrous dioxygen species are downhill and exothermic, and therefore these reactions should spontaneously proceed. Dioxygen activation is an essential driving force in P450-mediated alkane hydroxylation.

Acknowledgment. K.Y. acknowledges the Ministry of Culture, Sports, Science and Technology of Japan, the Japan Society for the Promotion of Science, the Iwatani Naoji Foundation, the Takeda Science Foundation, and Kyushu University P & P 'Green Chemistry' for their support of this work. Computations were in part carried out at the Computer Center of the Institute for Molecular Science.

JA0208862